AN ALGEBRAIC GEOMETRY PERSPECTIVE FOR THE ESTIMATION OF THE DIRECTIONS OF ARRIVAL

MARCO COMPAGNONI, ROBERTO NOTARI, MARCO MARCON, UMBERTO SPAGNOLINI

Abstract. Directions of Arrival for Uniform Linear Arrays represent a widely studied topic in many fields of signal processing, with large attention on computational complexity, estimation accuracy and noise rejection. In this article we study the mathematical model behind Directions of Arrival from the point of view of algebraic geometry, focusing on its relation with the rational normal curve. On this basis, we give a novel interpretation for the root-MUSIC algorithm, that is a widely adopted estimation approach in signal processing. Furthermore, we propose some novel estimation techniques. The first one is based on the computation of the points on the rational normal curve that minimize the distance from the linear subspace defined by the measured Directions of Arrival. The others require the study of the secant varieties of the rational normal curve and the minimization of the distance between the point of the Grassmannian defined by the signal subspace and a certain secant variety. The results obtained from simulations in a noisy scenario show that our estimators are statistically consistent. One algorithm outperforms root-MUSIC over a wide range of scenarios, especially in presence of few snapshots and low Signal to Noise Ratio.

1. Introduction

Smart Sensors Arrays (SSAs) are, nowadays, the basic component for many communication systems employing smart antennas for 5G networks [1], sensing systems with array of microphones [2] and radars [3]. For all these systems an accurate estimation of the Directions of Arrival (DoAs) is a crucial step for performance efficiency both in sources localization (for receiver systems) and for efficient signaling along a specific beam direction (for transmitter systems)[4]. Thanks to the adaptation of SSAs to multiple directions, it is possible to orient the radiation beam toward a specific direction or to separate the signal from different sources placed in different angular positions by avoiding interference and energy scattering in null directions [5].

The SSAs can assume different shapes, that usually trade among many factors, some of which are the maximum number of sensors, the Signal to Noise Ratio (SNR) and the Signal to Interference Ratio (SIR), the number of concurrent sources, and the opportunity to extend geometries from linear to planar and also volumetric arrays. In this manuscript, we focus on the study of Uniform Linear Arrays (ULAs), by employing techniques from algebraic geometry. This case is the fundamental array configuration that provides the basic insight for theoretical developments [6].

1.1. The steering vectors.

Let us consider the most general scenario, where there is a sensor array consisting of L sensors with a given spatial distribution and there are M sources in unknown position. Assuming a homogeneous medium, the physical world can

Date: October 9, 2022.

2020 *Mathematics Subject Classification.* 13P15,14H45,14N07,51M16,94A12.

Key words and phrases. Directions of arrival, rational normal curves, secant varieties, applied algebraic geometry.

be identified as the Euclidean space. After choosing an orthogonal Cartesian coordinate system, it can be identified as $\mathbb{R}^3$.

The positions of the sensors are $\mathbf{p_l}$, where $l = 1, \dots, L$. In typical applications, the sources are very distant from the sensors, in comparison to the array's size. Hence, the signals measured by the sensors are usually modeled as plane waves (see Fig. 1).

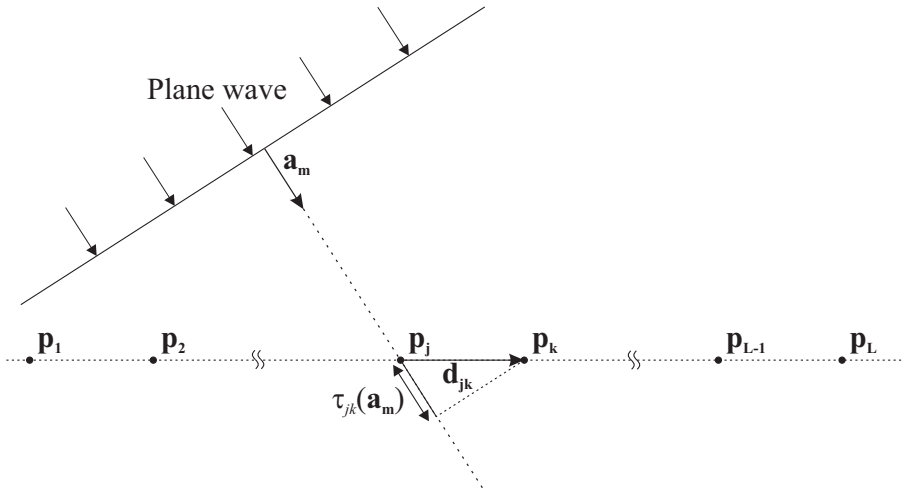

FIGURE 1. A plane wave with orientation $\mathbf{a_m}$ interacts with a ULA composed by L sensors in positions $\mathbf{p_1}, \dots, \mathbf{p_L}$. The delay $\tau_{jk}(\mathbf{a_m})$, assuming $c = 1$, is equal to the length of the projection of $\mathbf{d_{jk}}$ on $\mathbf{a_m}$.

This means that for every $m = 1, \dots, M$ there exists a propagation direction of the signal of the n-th source, described by a unit vector $\mathbf{a_m}$. In the DoA localization problems, the goal is to estimate these unknown vectors $\mathbf{a_m}$ from the signals measured by the array.

In the planar wave approximation, the signal emitted by the m-th source is constant on each plane perpendicular to $\mathbf{a_m}$, for any given time t. The wave front travels in space with velocity c. By considering the displacement vector $\mathbf{d_{jk}} = \mathbf{p_k} - \mathbf{p_j}$ from sensor j to sensor k, this implies that the time delay of the wave front between the two sensors is

$$\tau_{jk}(\mathbf{a_m}) = \frac{\langle \mathbf{d_{jk}}, \mathbf{a_m} \rangle}{c}. \tag{1}$$

On the plane of the wave front, the m-th signal can be described by a real vector perpendicular to $\mathbf{a_m}$. In order to streamline the notation, in signal processing it is usual to represent such a signal in terms of a complex-valued function $s_m(t)$ of the time t :

$$s_m(t) = g_m(t) \exp(i h_m(t)),$$

where $g_m(t)$ and $h_m(t)$ are real-valued functions and i is the imaginary unit. Common assumptions for most of SSAs applications are [7][8][9][10]:

- the signals are narrow-band with the same central frequency ω. This implies that:
$$h_m(t) = \omega t + \vartheta_m(t);$$
- the signals are slowly varying in time with respect to the planar wave period. This means that the amplitude and the phase associated to the signal can be considered constant for the whole time required to reach all sensors of the array, i.e. $g_m(t) \approx g_m(t + \tau_{jk}(\mathbf{a_m}))$ and $\vartheta_m(t) \approx \vartheta_m(t + \tau_{jk}(\mathbf{a_m}))$ for all possible values of $\tau_{jk}(\mathbf{a_m})$.

As a consequence, the only differences between the measurements of the same signal taken by two different sensors of the array at time t are phase terms, due to the propagation delays (1). More precisely, let $s_m(t)$ be the measurement taken at time t by the first sensor of the array and related to the signal emitted by the m-th source. Then

$$\begin{aligned} s_{m,l}(t) &= g_m(t-\tau_{1l}(\mathbf{a_m}))\exp(i\omega(t-\tau_{1l}(\mathbf{a_m}))+\vartheta_m(t-\tau_{1l}(\mathbf{a_m}))) \\ &\approx g_m(t)\exp(i\omega(t-\tau_{1l}(\mathbf{a_m}))+\vartheta_m(t)) = s_m(t)\exp(-i\omega\tau_{1l}(\mathbf{a_m})) \end{aligned} \tag{2}$$

is the signal measured at time t by the l-th sensor, for $l = 1, \ldots, L$.

Hence, the impinging signal on each element l of the array can be defined as the superposition of M planar waves, i.e.

$$x_l(t) = \sum_{m=1}^{M} s_{m,l}(t) = \sum_{m=1}^{M} s_m(t)\exp(-i\omega\tau_{1l}(\mathbf{a_m})). \tag{3}$$

Let us define in $\mathbb{C}^L$ the *array steering vector*, associated to the propagation direction $\mathbf{a_m}$:

$$\mathbf{h}(\mathbf{a_m}) = (1, \exp(-i\omega\tau_{12}(\mathbf{a_m})), \ldots, \exp(-i\omega\tau_{1L}(\mathbf{a_m}))).^{1} \tag{4}$$

From (3), it follows that the vector $\mathbf{x}(t) = (x_1(t), \ldots, x_L(t))$ of the L measurements taken by the sensors at time t is the following linear combination of the steering vectors:

$$\mathbf{x}(t) = \sum_{m=1}^{M} s_m(t)\ \mathbf{h}(\mathbf{a_m}). \tag{5}$$

1.2. **The geometric point of view.** When M noiseless signals from different fixed directions $\mathbf{a_1}, \ldots \mathbf{a_M}$ are impinging in a SSA, they define the vector $\mathbf{x}(t)$. This vector lies on the M-dimensional subspace of $\mathbb{C}^L$ generated by $\mathbf{h}(\mathbf{a_1}), \ldots, \mathbf{h}(\mathbf{a_M})$, that is named the *signal subspace* V. In the signal processing literature, the subset of $\mathbb{C}^L$ defined by the steering vectors $\mathbf{h}(\mathbf{a})$ for every possible direction of arrival $\mathbf{a}$ of the signal is referred to as the *array manifold* [8].

The geometric properties of the array manifold and the signal subspace have been studied by many authors in the engineering literature, mainly from a differential geometry standpoint [8]. In the case of planar localization (2D), the sources, the array and consequently the vector $\mathbf{a}$ lie on a plane. Hence, the array manifold is a parametric curve, where the natural parameter is the azimuth, i.e. the angle describing the orientation $\mathbf{a}$ of the plane wave with respect to a reference direction. In the general case of space localization problems (3D), the array manifold is a parametric surface. In such a scenario the natural parameters are azimuth and elevation, that denote the two physical angles describing the vector $\mathbf{a}$ with respect to a reference plane and direction.

In this paper, we work with the particular case of the array manifold associated with a ULA, from the point of view of algebraic geometry. This means that the array elements we are considering are equally spaced along a straight line. Hence, the array steering vector can be written as:

$$\mathbf{h}(\mathbf{a_m}) = \left(1, z_m, \ldots, z_m^{L-1}\right), \tag{6}$$

[1] In real applications, the *array steering vector* has a dependence from the impinging direction $\mathbf{a_m}$ also from a complex response $\zeta_m(\mathbf{a_m}, \omega)$, due to the non-isotropic behavior of the transducer. This means that:

$$\mathbf{h}(\mathbf{a_m}) = (\zeta_1(\mathbf{a_m}, \omega), \zeta_2(\mathbf{a_m}, \omega)\exp(-i\omega\tau_{12}(\mathbf{a_m})), \ldots, \zeta_L(\mathbf{a_m}, \omega)\exp(-i\omega\tau_{1L}(\mathbf{a_m}))).$$

However, this deterministic effect can be handled and corrected *a posteriori*, therefore we disregard it in our analysis.

where $z_m = \exp(-i\omega\tau_{12}(\mathbf{a_m}))$. In this setting, the array manifold is a parametric curve, both in the 2D and 3D localization problems. Indeed, by measuring the phases of the signal among sensors, we can only determine the angle between the line containing the array and the orientation $\mathbf{a}$ of the plane wave. This means that in 2D localization one can only find the orientation up to a reflection with respect to the array line, while in 3D localization one can only find the half-cone, having the array line as axis, on which the vector $\mathbf{a}$ lies.

1.3. **Structure of the manuscript.** In this manuscript, we study the estimation problem of the DoAs with a ULA of sensors. The structure of the work is the following.

In Section 2 we study the deterministic model, i.e. in absence of noise, for the DoAs. In particular, we relate the signal subspace to the image of a particular linear function and we show that the array manifold is a subset of the rational normal curve. Based on that, we also give some algebraic and geometrical results that will be useful for the localization problem.

In Section 3 we focus on the estimation problem in presence of noisy measurements. Most of the DoAs estimation methods can be divided into two large classes: classical approaches not based on subspace analysis and the ones based on subspace analysis. The former methods are based on Capon or Minimum Variance Distortionless Response (MVDR) [11] approach. MVDR methods are usually computationally demanding due a full-rank matrix inversion even if GPU computing made feasible their use also for real time applications [12]. In this manuscript we focus on the latter type of methods, that are based on different approaches for subspace analysis [13]. We present the classical root-MUSIC algorithm and we give a clear geometric interpretation of it. Then, we define a new estimation method based on our previous geometric analysis of the deterministic problem.

In Section 4 we present the secant varieties of the rational normal curve. We show the relation between the estimation of M DoAs and the geometry of the M–secant variety of M–subspaces of $\mathbb{C}^L$ to the rational normal curve. This allows us to define novel estimation methods for the DoAs.

In Section 5 we apply our proposals to an explicit example of DoAs estimation. Although this is a preliminary analysis, it shows that our methods give results that are compatible with the ones of root-MUSIC.

In Section 6 we further investigate the performances of our estimators. A simulation campaign shows that one of the proposed algorithm outperforms root-MUSIC, especially in presence of a low number of snapshots and low SNR.

Finally, Section 7 draws some conclusions and describes future research directions that can take advantage of the analysis presented in this paper.

In order to keep the paper as self-contained as possible, in Appendix A we give an overview on projective geometry, on the rational normal curve, Grassmannians and secant varieties. This section, of course, can be skipped by readers who are already familiar with these topics. Finally, in Appendix B there are the more technical computations that allow the simplification of the polynomial systems appearing in Section 5.

2. The deterministic DoA model

2.1. **The steering map, the array manifold and the signal subspace for a ULA.** As explained in Section 1.1, in a noiseless scenario the SSA response vector $\mathbf{x}(t)$ is a linear combination of the steering vectors $\mathbf{h}(\mathbf{a_1}), \dots, \mathbf{h}(\mathbf{a_M})$, with complex coefficients given by

the signals $s_1(t), \dots, s_M(t)$ measured by the first sensor of the array. We can reformulate the question in terms of a certain linear function.

Definition 1. *Let $\alpha_1, \dots, \alpha_M$ be distinct real numbers in $[0, 2\pi)$ and $z_m = \exp(-i\alpha_m)$, for every $m = 1, \dots, M$. The steering map associated to $\alpha_1, \dots, \alpha_M$ is the linear function $\varphi : \mathbb{C}^M \to \mathbb{C}^L$ defined on the standard basis $(\mathbf{e_1}, \dots, \mathbf{e_M})$ of $\mathbb{C}^M$ as*

$$\varphi(\mathbf{e_m}) = (1, z_m, \dots, z_m^{L-1}), \qquad \text{for every} \qquad m = 1, \dots, M.$$

If $\alpha_m = \omega\tau_{12}(\mathbf{a_m})$ for every $m = 1, \dots, M$, then $\varphi(\mathbf{e_m}) = \mathbf{h}(\mathbf{a_m})$. Let us define the signal vector $\mathbf{s}(t) = (s_1(t), \dots, s_M(t))$ in $\mathbb{C}^M$, therefore

$$\mathbf{x}(t) = \varphi(\mathbf{s}(t)).$$

It follows that the signal subspace V coincides with the image $\mathrm{Im}(\varphi)$ of the steering map. To simplify the notation, we set $\mathbf{h_m} = \varphi(\mathbf{e_m})$ for every $m = 1, \dots, M$. These vectors satisfy the following results.

Lemma 1. *The vectors $\mathbf{h_1}, \dots, \mathbf{h_M}$ are linearly independent with module $\sqrt{L}$. The subspace spanned by each one of them is a point in $\mathbb{P}^L_{\mathbb{C}}$ that belongs to the rational normal curve[2] $C \subseteq \mathbb{P}^L_{\mathbb{C}}$.*

Proof. Let us remind that $\mathbf{h_m} = (1, z_m, \dots, z_m^{L-1})$. Since $z_m\overline{z_m} = 1$ for every $m = 1, \dots, M$, it follows that $\mathbf{h_m}$ has module $\sqrt{L}$. Furthermore, the homogeneous coordinates of the subspace spanned by $\mathbf{h_m}$ are $[1 : z_m : \cdots : z_m^{L-1}]$. This is the point $v_{L-1}([1 : z])$ of the rational normal curve C, where v_{L-1} is the Veronese embedding of $\mathbb{P}^1_{\mathbb{C}}$ into $\mathbb{P}^{L-1}_{\mathbb{C}}$. Finally, $\mathbf{h_1}, \dots, \mathbf{h_M}$ are linearly independent because $\alpha_1, \dots, \alpha_M$ are pairwise different (see Proposition 8). □

From now on, by abuse of notation we will identify an element in a vector space with the corresponding point in the associated projective space. Furthermore, whenever useful, we will also identify a vector with the corresponding point in the associated affine space.

Theorem 1. *The vectors $\mathbf{h_1}, \dots, \mathbf{h_M}$ are the intersection points of the image $Im(\varphi)$ and the rational normal curve C.*

Proof. By definition, $\mathbf{h_1}, \dots, \mathbf{h_M}$ are in $\mathrm{Im}(\varphi)$. On the other hand, Lemma 1 states that they lie on C. Moreover, from the same lemma it follows that the steering map φ is injective, therefore the dimension of $\mathrm{Im}(\varphi)$ is equal to M. Since a linear subspace W intersects the rational normal curve in at most $\dim(W)$ points, then $\mathbf{h_1}, \dots, \mathbf{h_M}$ are the intersection points of $\mathrm{Im}(\varphi)$ and C.[3] □

These results show us that the array manifold for a ULA is a subset of the rational normal curve.

2.2. **The deterministic localization problem.** Let $\mathbf{x_1}, \dots, \mathbf{x_N}$ be N noiseless measurements vectors taken at different time by the ULA. It is possible to locate the M sources if and only if one can compute all the steering vectors $\mathbf{h_1}, \dots, \mathbf{h_M}$ starting from the measured data. This problem is equivalent to determine the steering map φ and it has a unique solution if and only if $\mathbf{x_1}, \dots, \mathbf{x_N}$ span $\mathrm{Im}(\varphi)$. In such a case, the solution of the deterministic DoA problem can be obtained as follows.

Let $\mathbf{X}$ be the $L \times N$ matrix whose columns are given by the components of the vectors $\mathbf{x_1}, \dots, \mathbf{x_N}$. By hypothesis, $\mathbf{X}$ has rank M. Let $(\mathbf{u_1}, \dots, \mathbf{u_{L-M}})$ be an orthonormal basis

[2]See Section A for the definition and properties of projective spaces and rational normal curves.

[3]In this manuscript, we only use dimension in the vector space or affine sense.

of the orthogonal complement $V^\perp$ of the signal space $V = \mathrm{Im}(\varphi)$, with respect to the Hermitian scalar product. We name $\mathbf{U}$ the $L \times (L-M)$ matrix of rank $L-M$ whose columns are given by the components of these vectors. It follows that $\mathbf{U}^H\mathbf{X} = 0$, where $\mathbf{U}^H$ is the Hermitian conjugate of $\mathbf{U}$.

Thus, the components of vectors $\mathbf{z}$ in $\mathrm{Im}(\varphi)$ are solutions of the homogeneous linear system associated to the matrix $\mathbf{U}^H$. By requiring that $\mathbf{z}$ stays also on C, we have $\mathbf{z} = (1, z, \dots, z^{L-1})$. Thus, we get a system of polynomial equations, or equivalently, an ideal in the polynomial ring $\mathbb{C}[z]$. Because of Theorem 1, this ideal is generated by the unique monic polynomial of degree M :

$$p(z) = c_0 + \cdots + c_{M-1}z^{M-1} + z^M \tag{7}$$

whose roots are $z_1, \dots, z_M$. By setting

$$\mathbf{Z} = \begin{bmatrix} 1 \\ z \\ \vdots \\ z^{L-1} \end{bmatrix},$$

we have the following results.

Proposition 1. *The polynomial $p(z)$ is the greatest common divisor of the polynomials obtained as rows of $\mathbf{U}^H\mathbf{Z}$.*

Proof. The statement follows from the fact that $\mathbb{C}[z]$ is a principal ideal domain and from Theorem 1. □

Remark 1. If the minor of $\mathbf{U}^H$ corresponding to the last $L-M$ columns is non-zero, then the polynomial $p(z)$ can be obtained by Gaussian elimination from $\mathbf{U}^H$. In geometrical terms, this procedure corresponds to look for the unique $(L-1)$-dimensional linear space that intersects the rational normal curve C at points $\mathbf{h_1}, \dots, \mathbf{h_M}$ and at the ideal point $v_{L-1}([0:1]) = [0:\cdots:0:1]$ with multiplicity $L-M$. Since we are working in an affine setting, the ideal point simply disappears. This approach has been pursued in [14], although in that paper there is no explanation of such a procedure in terms of intersection of $\mathrm{Im}(\varphi)$ and C.

By summarizing the deterministic DoA model, we can say that to determine the steering map and find the directions $\mathbf{a_1}, \dots, \mathbf{a_M}$, it is enough to intersect the linear span of the data $\mathbf{x_1}, \dots, \mathbf{x_N}$ with the rational normal curve.

2.3. **Further properties of the array manifold.** We close the section by giving a result that will be useful later.

Proposition 2. *Let us consider the polynomial*

$$q(z) = \mathbf{Z}^T\mathbf{J}\mathbf{U}\mathbf{U}^H\mathbf{Z}, \qquad \textit{where} \qquad \mathbf{J} = \begin{bmatrix} 0 & \dots & 1 \\ \vdots & \iddots & \vdots \\ 1 & \dots & 0 \end{bmatrix}. \tag{8}$$

If $z = \exp(-i\alpha)$, then the Hermitian squared distance of $\mathbf{z} = (1, z, \dots, z^{L-1})$ from the signal subspace V is the rational function

$$d(\mathbf{z}, V)^2 = \frac{q(z)}{z^{L-1}}.$$

Proof. The components of the orthogonal projection of $\mathbf{z}$ onto $V^\perp$ are

$$\mathbf{P}_{\mathbf{V}^\perp}(z) = \mathbf{U}\mathbf{U}^H \begin{bmatrix} 1 \\ z \\ \vdots \\ z^{L-1} \end{bmatrix}.$$

Therefore, the squared distance from $\mathbf{z}$ to V is

$$d(\mathbf{z}, V)^2 = \|\mathbf{P}_{\mathbf{V}\perp}(z)\|^2 = \begin{bmatrix} 1 & \overline{z} & \dots & \overline{z}^{L-1} \end{bmatrix} \mathbf{U}\mathbf{U}^H \begin{bmatrix} 1 \\ z \\ \vdots \\ z^{L-1} \end{bmatrix},$$

where $\overline{z}$ is the complex conjugate of z. However, $\overline{z} = 1/z$ and so the statement follows. □

Because of its geometrical interpretation, it is evident that $q(z_m) = 0$ for every $m = 1, \dots, M$, where z_m is a root of $p(z)$. Thus, $q(z)$ is a multiple of $p(z)$. We can go further with this analysis.

Lemma 2. *If $z = \exp(-i\alpha)$, then*

$$\overline{p(z)} = \frac{1}{c_0 z^M} p(z).$$

Proof. The roots of $p(z)$ are $z_1, \dots, z_M$, with $z_m = \exp(-i\alpha_m)$ for $m = 1, \dots, M$. Let us assume that $z = \exp(-i\alpha)$. We have:

$$\begin{aligned} \overline{p(z)} &= \overline{(z - z_1) \cdots (z - z_M)} = (\overline{z} - \overline{z_1}) \cdots (\overline{z} - \overline{z_M}) = \\ &= \left(\frac{1}{z} - \frac{1}{z_1}\right) \cdots \left(\frac{1}{z} - \frac{1}{z_M}\right) = \frac{1}{z_1 \cdots z_M z^M} (-1)^M p(z) = \frac{1}{c_0 z^M} p(z), \end{aligned}$$

since $c_0 = (-1)^M z_1 \cdots z_M$, as follows from Newton's identities. □

Corollary 1. *z_m is a root of $q(z)$ with multiplicity at least two, for every $m = 1, \dots, M$.*

Proof. We give two different proofs of the statement, since each one of the two proofs highlights and uses different properties.

(1) The polynomial $p(z)$ is the greatest common divisor of the polynomials in $\mathbf{U}^H\mathbf{Z}$, hence there exists a $(L - M) \times (L - M - 1)$ matrix $\mathbf{A}$ over $\mathbb{C}$ such that

$$\mathbf{U}^H\mathbf{Z} = p(z)\mathbf{A}^H\overline{\mathbf{Z}},$$

where $\overline{\mathbf{Z}} = [1 \ z \ \dots \ z^{L-M-1}]^T$. Since $d(z, V)^2 = (\mathbf{U}^H\mathbf{Z})^H(\mathbf{U}^H\mathbf{Z})$, we get

$$d(z, V)^2 = \overline{p(z)}\, p(z)\, \overline{\mathbf{Z}}^H \mathbf{A}\mathbf{A}^H\overline{\mathbf{Z}}.$$

From Lemma 2, it follows

$$q(z) = p(z)^2 \frac{1}{c_0} \overline{\mathbf{Z}}^T \mathbf{J_1} \mathbf{A}\mathbf{A}^H\overline{\mathbf{Z}},$$

where $\mathbf{J_1}$ is the order $L - M - 1$ square submatrix of $\mathbf{J}$ obtained by removing the last M rows and the first M columns.

(2) By definition, $\mathbf{h_m} = (1, z_m, \dots, z_m^{L-1})$ is a generator of V. Hence, $d(\mathbf{h_m}, V) = 0$ and consequently $q(z_m) = 0$. Furthermore, let us consider the derivative of $q(z)$:

$$\frac{d}{dz}q(z) = \left(\frac{d}{dz}\mathbf{Z}^T\right)\mathbf{J}\mathbf{U}\mathbf{U}^H\mathbf{Z} + \mathbf{Z}^T\mathbf{J}\mathbf{U}\mathbf{U}^H\left(\frac{d}{dz}\mathbf{Z}\right) = \\ = \left(\frac{d}{dz}\mathbf{Z}^T\right)\mathbf{J}\mathbf{P}_{\mathbf{V}^\perp}(z) + z^{L-1}\,\mathbf{P}_{\mathbf{V}^\perp}(1/\overline{z})^H\left(\frac{d}{dz}\mathbf{Z}\right).$$

If we evaluate the previous expression at z_m, we obtain $\mathbf{P}_{\mathbf{V}^\perp}(z_m) = 0$ and $\mathbf{P}_{\mathbf{V}^\perp}(1/\overline{z_m}) = \mathbf{P}_{\mathbf{V}^\perp}(z_m) = 0$. It follows that z_m is a zero of the derivative of $q(z)$, therefore it is a root with multiplicity at least 2 of $q(z)$.

□

The first proof gives us the quotient of the division between $q(z)$ and $p(z)^2$ in terms of the data. The second proof, instead, allows us to get an approximation via Taylor formula of $q(z)$.

3. The noisy DoA model

In real applications, the data are affected by noise. The measurements vectors $\mathbf{y_1}, \dots, \mathbf{y_N}$ can be written as sum of the deterministic vectors $\mathbf{x_1}, \dots, \mathbf{x_N}$ and the impairments $\boldsymbol{\epsilon_1}, \dots, \boldsymbol{\epsilon_N}$:

$$\mathbf{y_i} = \mathbf{x_i} + \boldsymbol{\epsilon_i} \qquad \text{for} \qquad i = 1, \dots, N.$$

It is common to assume $N \geq M$ and the noise as a stochastic stationary process independent from the signal, with a zero-mean Gaussian distribution.

3.1. Root-MUSIC.

In this section, we summarize root-MUSIC. This is a classical algorithm, based on the subspace analysis, for estimating the DoAs in presence of noisy measurements. Many variations and implementations of root-MUSIC have been proposed in literature ([15],[16],[17],[18]) tackling different aspects and applications of the algorithm.

For the sake of simplicity, we assume to know in advance the number M of sources. The root-MUSIC method works with a two step procedure. Firstly, it estimates the signal subspace $\widehat{V}$ as the M–dimensional linear subspace of $\mathbb{C}^L$ that best fits the data $\mathbf{y_1}, \dots, \mathbf{y_N}$. Then, it computes a suitable polynomial among whose roots one finds the M DoAs.

In the first step of root-MUSIC, one applies the Principal Component Analysis (PCA) to $\mathbf{y_1}, \dots, \mathbf{y_N}$. Because of our assumptions on the deterministic measurement $\mathbf{x}$ and the error $\boldsymbol{\epsilon}$, the expected values of the real measurements $\mathbf{y} = \mathbf{x} + \boldsymbol{\epsilon}$ define an affine subspace of $\mathbb{C}^L$ that contains $\mathbf{0}$. Therefore, the PCA is simplified. Let us define the $L \times N$ data matrix $\mathbf{Y}$, whose columns are given by the components of $\mathbf{y_1}, \dots, \mathbf{y_N}$. The covariance matrix of $\mathbf{Y}$ is the Hermitian matrix $\mathbf{R_Y} = \mathbf{Y}\mathbf{Y}^H$ of order L, that has non-negative real eigenvalues $\lambda_1 \geq \dots \geq \lambda_L \geq 0$. Then, the estimated signal subspace is $\widehat{V} = V_{\lambda_1} \oplus \dots \oplus V_{\lambda_M}$, where V_{λ_l} is the eigenspace associated to the l-th eigenvalue. From a geometric point of view, it is well known that $\widehat{V}$ can be thought of as the M dimensional affine subspace of $\mathbb{C}^L$ that minimizes the sum of the squared distances from $\mathbf{y_1}, \dots, \mathbf{y_N}$.

In the second step, root-MUSIC takes in consideration the subspace orthogonal to $\widehat{V}$, that is $\widehat{V}^\perp = V_{\lambda_{M+1}} \oplus \dots \oplus V_{\lambda_L}$. The unit eigenvectors corresponding to the smallest $L - M$ eigenvalues of $\mathbf{R_Y}$ define a basis of $\widehat{V}^\perp$. The matrix $\widehat{U}$ whose columns are the components of these eigenvectors is the root-MUSIC estimation of the matrix U of Section 2.2. Thus, the polynomial

$$\widehat{q}(z) = \mathbf{Z}^T\mathbf{J}\widehat{\mathbf{U}}\widehat{\mathbf{U}}^H\mathbf{Z} \tag{9}$$

is the root-MUSIC estimation of $q(z)$, defined in Proposition 2. If the noise is not too large, Corollary 1 implies that $\widehat{q}(z)$ has M pairs of roots that approximately are given by reciprocal complex numbers, whose modules are close to 1. By the mean of each pair, one obtains the estimation of $z_1, \dots, z_M$, and so the estimation of the DoAs $\mathbf{a_1}, \dots, \mathbf{a_M}$.

3.2. **Minimum Distance on the Curve.** On the base of our geometric interpretation of the DoA localization problem, now we propose a novel estimation algorithm for the DoA of the signals. At this aim, we give a theoretical result on the Hermitian distance between the points on the rational normal curve and affine subspaces of $\mathbb{C}^L$. Firstly, we remind that if V is such a generic subspace and $\mathbf{U}$ is a matrix whose columns are given by an orthonormal basis of its orthogonal complement, then the squared distance of the point $\mathbf{z} = (1, z, \dots, z^{L-1})$ with $z = \exp(-i\alpha)$ can be computed as

$$d(\mathbf{z}, V)^2 = \frac{1}{z^{L-1}} \mathbf{ZJUU}^H\mathbf{Z}\,.$$

Then, we define the following $L \times L$ diagonal matrix

$$\mathbf{K} = \begin{bmatrix} 0 & 0 & \dots & 0 \\ 0 & 1 & \dots & 0 \\ \vdots & \vdots & \ddots & \vdots \\ 0 & 0 & \dots & L-1 \end{bmatrix}$$

and the generalized commutator between two matrices

$$[\mathbf{A}, \mathbf{B}]_k = \begin{cases} \mathbf{AB} - \mathbf{BA} & \text{if } k = 1, \\ [\mathbf{A}, [\mathbf{A}, \mathbf{B}]_{k-1}] & \text{if } k > 1. \end{cases}$$

The following identity holds:

$$\frac{d}{dz}\mathbf{Z} = \frac{1}{z}\mathbf{KZ}.$$

Lemma 3. *Let us take $z = \exp(-i\alpha)$ and $\mathbf{z} = (1, z, \dots, z^{L-1})$. The k-th derivative of the Hermitian squared distance $d(\mathbf{z}, V)^2$ with respect to α is the rational function*

$$\frac{d^k}{d\alpha^k}\, d(\mathbf{z}, V)^2 = \frac{i^k}{z^{L-1}}\, \mathbf{Z}^T J\, [\mathbf{K}, \mathbf{UU}^H]_k\, \mathbf{Z}. \tag{10}$$

Proof. Let us take the function

$$f(\alpha) = \frac{1}{z^{L-1}}\, \mathbf{Z}^T\mathbf{JAZ},$$

where $\mathbf{A}$ is a generic $L \times L$ matrix. Using Proposition 2, when $\mathbf{A} = \mathbf{UU}^H$ this function is the Hermitian squared distance. We have:

$$\frac{d}{d\alpha} f(\alpha) = -iz\, \frac{d}{dz} \left(\frac{1}{z^{L-1}}\, \mathbf{Z}^T\mathbf{JAZ} \right) = \frac{i}{z^{L-1}} \left((L-1)\mathbf{Z}^T\mathbf{JAZ} - z\, \frac{d}{dz} \left(\mathbf{Z}^T\mathbf{JAZ} \right) \right).$$

Let us focus on the second term in the bracket:

$$\begin{aligned} z\, \frac{d}{dz} \left(\mathbf{Z}^T\mathbf{JAZ} \right) &= \left(z\, \frac{d}{dz}\mathbf{Z}^T \right) \mathbf{JAZ} + \mathbf{Z}^T\mathbf{JA} \left(z\, \frac{d}{dz}\mathbf{Z} \right) = \\ &= \mathbf{Z}^T\mathbf{KJAZ} + \mathbf{Z}^T\mathbf{JAKZ} = \mathbf{Z}^T \left(\mathbf{KJA} + \mathbf{JAK} \right) \mathbf{Z}. \end{aligned}$$

It follows that:

$$\frac{d}{d\alpha}f(\alpha) = \frac{i}{z^{L-1}}\mathbf{Z}^T\left((L-1)\mathbf{JA} - \mathbf{KJA} - \mathbf{JAK}\right)\mathbf{Z} = \\ = \frac{i}{z^{L-1}}\mathbf{Z}^T\mathbf{J}\left(\left((L-1)\mathbf{I} - \mathbf{JKJ}\right)\mathbf{A} - \mathbf{AK}\right)\mathbf{Z} = \frac{i}{z^{L-1}}\mathbf{Z}^T\mathbf{J}\left[\mathbf{K}, \mathbf{A}\right]_1\mathbf{Z},$$

where $\mathbf{I}$ is the identity matrix and we used the identities

$$\mathbf{J}^2 = \mathbf{I} \qquad \text{and} \qquad (L-1)\mathbf{I} - \mathbf{JKJ} = \mathbf{K}.$$

By applying this formula to the Hermitian squared distance recursively, it is straightforward to prove the lemma. □

Proposition 3. *Let us take $z = \exp(-i\alpha)$ and $\mathbf{z} = (1, z, \dots, z^{L-1})$. The local minimum points of the Hermitian squared distance $d(\mathbf{z}, V)^2$ are the unitary roots of the polynomial*

$$r(z) = \mathbf{Z}^T\mathbf{J}\left[\mathbf{K}, \mathbf{U}\mathbf{U}^H\right]_1\mathbf{Z} \tag{11}$$

that satisfy

$$\frac{d^2}{d\alpha^2}\, d(\mathbf{z}, V)^2 = -\frac{1}{z^{L-1}}\,\mathbf{Z}^T\mathbf{J}\left[\mathbf{K}, \mathbf{U}\mathbf{U}^H\right]_2\mathbf{Z} > 0. \tag{12}$$

Proof. The statement is a direct consequence of Lemma 3. □

The idea behind the Minimum Distance on the Curve (MDC) algorithm is to estimate the DoAs by searching for the M unit complex numbers z that define the M closest points on the rational normal curve to the estimated signal subspace. We achieve this result with the following steps:

Algorithm 1 Minimum Distance on the Curve (MDC)

1: compute the estimation $\widehat{V}$ of the signal subspace via PCA;
2: construct the polynomial $\widehat{r}(z)$ as in Proposition 3;
3: compute the unit roots of $\widehat{r}(z)$ that satisfy inequality (12);
4: among the previous roots, select the M ones that minimize the Hermitian distance. Finally, compute the estimation of the DoAs.

4. Secant varieties and the DoA problem

In this section, we show how the deterministic and the noisy DoA problems can be reformulated in terms of the M–secant variety of M–subspaces of $\mathbb{C}^L$ to the rational normal curve. We refer the reader to Appendix A for a quick survey on the topic.

4.1. **The deterministic problem.**

In order to solve the deterministic DoA problem, we have to compute the M intersection points of the rational normal curve C and the image of the steering map φ. The latter is V, an M–dimensional subspace of $\mathbb{C}^L$. Hence, V is a point of the secant variety $\mathcal{V}_{M,M}(C) \subset \mathbb{G}(M, \mathbb{C}^L)$, and we want to compute the M distinct points on the rational normal curve that span V.

Proposition 4. *Let $P_1, \dots, P_M$ be points on the rational normal curve C, whose coordinates are $(1 : u_m : \dots : u_m^{L-1})$, pairwise different. Let $(\dots : p_{m_1,\dots,m_M} : \dots)$ be the Plücker coordinates of the subspace spanned by $P_1, \dots, P_M$. Then,*

$$p(z) = \sum_{m=0}^{M} p_{0,\dots,\widehat{m},\dots,M} z^m \tag{13}$$

has $u_1, \dots, u_M$ as roots, where $\widehat{m}$ means that m is canceled from the set $\{0, \dots, M\}$.

Proof. The matrix

$$\mathbf{A} = \begin{bmatrix} 1 & u_1 & \dots & u_1^M \\ 1 & u_2 & \dots & u_2^M \\ \vdots & \vdots & & \vdots \\ 1 & u_M & \dots & u_M^M \end{bmatrix}$$

has rank M, since the determinant of the submatrix of the first M columns is Vandermonde. Therefore, the non-zero solutions of the linear system $\mathbf{AX} = \mathbf{0}$ are all proportional each other. The Plücker coordinates $p_m = p_{0,\dots,\widehat{m},\dots,M}$ verify the equality

$$\mathbf{A} \begin{bmatrix} p_0 \\ \vdots \\ p_M \end{bmatrix} = \mathbf{0}.$$

This means that $p_0 + p_1 u_m + \dots + p_M u_m^M = 0$ for every $m = 1, \dots, M$. Hence, the polynomial $p(z) = p_0 + p_1 z + \dots + p_M z^M$ has $u_1, \dots, u_M$ as roots. □

Since $p_M \neq 0$, we can divide $p(z)$ by p_M, and we get the only monic generator described in (7). Therefore, the solution of the deterministic DoA problem can be obtained through the following steps:

Algorithm 2 Plücker method

1: compute the Plücker coordinates of V;
2: construct the polynomial $p(z)$ as in Proposition 4;
3: compute the roots of $p(z)$.

Because of Definition 1, all the roots of $p(z)$ have modulo 1.

Finally, let us observe that this method can be applied as well to a scenario with noisy measurements. In this case, we obtain a polynomial $\widehat{p}(z)$ whose roots $\widehat{z}_1, \dots, \widehat{z}_M$ are an estimation of the noiseless roots. From them, we get an estimation of the M DoAs.

4.2. **The noisy problem.** Based on the previous results, now we propose alternative estimation criteria for the DoA localization problem in presence of noisy measurements, that have neat geometric interpretation. In this case, we need some theoretical results on the distance of a point in the Grassmannian from the secant variety.

4.2.1. *Fubini-Study Minimum Distance from the Secant Variety.* Since we are working in a projective space, we first use the Fubini-Study distance (see Appendix A). As in the previous subsection, let us take M distinct points $P_1, \dots, P_M$ on the rational normal curve C, corresponding to the vectors $\mathbf{u_1} = (1, u_1, \dots, u_1^{L-1}), \dots, \mathbf{u_M} = (1, u_M, \dots, u_M^{L-1})$. They generate an M-dimensional linear subspace of $\mathbb{C}^L$, that corresponds to a point P on the secant variety $\mathcal{V}_{M,M}(C)$, with Plücker coordinate given by $\mathbf{u_1} \wedge \dots \wedge \mathbf{u_M}$. If we take another point Q of the Grassmannian, whose homogeneous coordinates are $\mathbf{v} = (v_0, \dots, v_{L'})$, with $L' = \binom{L}{M} - 1$, the Fubini-Study distance between them is

$$d(P, Q) = \arccos\left(\frac{|\langle \mathbf{v}, \mathbf{u_1} \wedge \dots \wedge \mathbf{u_M} \rangle|}{\|\mathbf{v}\| \|\mathbf{u_1} \wedge \dots \wedge \mathbf{u_M}\|} \right).$$

Proposition 5. *Let us assume that* $\mathbf{v}$ *is a fixed nonzero vector. The restriction of the function*

$$f(u_1,\dots,u_M)=\frac{|\langle \mathbf{v},\mathbf{u_1}\wedge\cdots\wedge\mathbf{u_M}\rangle|^2}{\|\mathbf{v}\|^2\|\mathbf{u_1}\wedge\cdots\wedge\mathbf{u_M}\|^2}$$

on $|u_1|=\cdots=|u_M|=1$ *is a rational function*

$$f(u_1,\dots,u_M)=\frac{g(u_1,\dots,u_M)}{h(u_1,\dots,u_M)}.$$

The points P *of* $\mathcal{V}_{M,M}(C)$*, satisfying* $|u_1|=\cdots=|u_M|=1$*, and that minimize the Fubini-Study distance* $d(P,Q)$*, are solutions of the following polynomial system:*

$$\left\{\begin{array}{rcl} g(u_1,\dots,u_M)\,h_1(u_1,\dots,u_M)-h(u_1,\dots,u_M)\,g_1(u_1,\dots,u_M) & = & 0\\ & \vdots & \\ g(u_1,\dots,u_M)\,h_M(u_1,\dots,u_M)-h(u_1,\dots,u_M)\,g_M(u_1,\dots,u_M) & = & 0\end{array}\right., \tag{14}$$

where $g_m(u_1,\dots,u_M)$ *and* $h_m(u_1,\dots,u_M)$ *are the partial derivatives of* g,h *with respect to* u_m*, for* $m=1,\dots,M$*.*

Proof. By the same reasoning behind the proofs of Proposition 2 and Lemma 3, the constraints imply that $\overline{u}_m=1/u_m$ for every $m=1,\dots,M$. As a consequence, the function $f(u_1,\dots,u_M)$ is rational. If $u_m=\exp(-i\alpha_m)$ for $m=1,\dots,M$, then we can think to f as a real function of $\alpha_1,\dots,\alpha_M$. Its partial derivatives are:

$$\frac{\partial}{\partial_{\alpha_m}}f(\alpha_1,\dots,\alpha_M)=\frac{iu_m}{h(u_1,\dots,u_M)^2}\cdot \\ (g(u_1,\dots,u_M)\,h_m(u_1,\dots,u_M)-h(u_1,\dots,u_M)\,g_m(u_1,\dots,u_M))$$

for $m=1,\dots,M$. Because of the constraints, the stationary points of $f(\alpha_1,\dots,\alpha_M)$ must satisfy the polynomial system (14).

Finally, the second statement of the proposition follows from the fact that arccosine and square root are monotonic functions. This means that the extremum points of $f(\alpha_1,\dots,\alpha_M)$ and $d(P,Q)$ coincide. □

It is not difficult to show that the minimum points of $d(P,Q)$ are the maximum points of $f(\alpha_1,\dots,\alpha_M)$. Moreover, the latter function is bounded from above by 1, because of the Cauchy-Schwarz inequality.

Now we are ready to formulate the Fubini-Study Minimum Distance from the Secant Variety (FSMDSV) estimation algorithm for the DoAs. In this case, the idea is to search for the point P of the secant variety $\mathcal{V}_{M,M}(C)$ that is closest to the point Q of the Grassmannian corresponding to the estimated signal subspace. We have the following steps:

Algorithm 3 Fubini-Study Minimum Distance from the Secant Variety (FSMDSV)

1: compute the estimation $\widehat{V}$ of the signal subspace via PCA and compute the Plücker coordinates defining Q;
2: construct the polynomial system (14) as in Proposition 5;
3: compute the solutions of (14) given by M-tuple of distinct complex numbers $(u_1,\dots,u_M)$ with modulus 1;
4: among the previous solutions, select the point P that minimize the Fubini-Study distance, or equivalently such that the value of f is closest to 1. Finally, compute the estimation of the DoAs.

4.2.2. *Hermitian Minimum Distance from the Secant Variety.* On the same line, we present a further method to solve the DoA estimation problem. As above, $P_1, \dots, P_M$ are pairwise different points on the rational normal curve C. They correspond to the vectors $\mathbf{u_1} = (1, u_1, \dots, u_1^{L-1}), \dots, \mathbf{u_M} = (1, u_M, \dots, u_M^{L-1})$, where $u_1, \dots, u_M$ are complex numbers with modulus 1. Hence, the point $\mathbf{u_1} \wedge \cdots \wedge \mathbf{u_M}$ belongs to the open set $p_{0,\dots,M-1} \neq 0$ of the projective space $\mathbb{P}^{L'}$. We identify such an open subset with the affine space $\mathbb{A}^{L'}$ by means of the map $\pi : \mathbb{P}^{L'} \setminus H \to \mathbb{A}^{L'}$, where H is the hyperplane $p_{0,\dots,M-1} = 0$. Then, $\pi(\mathbf{u_1} \wedge \cdots \wedge \mathbf{u_M})$ is a point in $\mathbb{A}^{L'}$ whose coordinates are polynomials in $u_1, \dots, u_M$, thanks to the following Lemma.

Lemma 4. *Let $P_1, \dots, P_M$ be points on the rational normal curve C, whose coordinates are $\mathbf{u_i} = (1 : u_i : \cdots : u_i^{L-1})$, pairwise different, and let $(\cdots : p_{i_1,\dots,i_M} : \dots)$ be the Plücker coordinates of the subspace spanned by $P_1, \dots, P_M$. Then*

$$\frac{p_{i_1,\dots,i_M}}{p_{0,\dots,M-1}} = s_{i_1,\dots,i_M}(u_1, \dots, u_M),$$

where $s_{i_1,\dots,i_M}$ is a symmetric polynomial in $u_1, \dots, u_M$.

Proof. See [19]. □

Let us take another point Q in $\mathbb{P}^{L'} \setminus H$, whose homogeneous coordinates are $\mathbf{v} = (v_0, \dots, v_{L'})$. Then, we can compute the Hermitian distance between $\pi(\mathbf{u_1} \wedge \cdots \wedge \mathbf{u_M})$ and $\pi(\mathbf{v})$ in $\mathbb{A}^{L'}$.

Proposition 6. *Let us assume that $\mathbf{v}$ is a fixed nonzero vector in $\mathbb{P}^{L'} \setminus H$. The restriction of the function*

$$f(u_1, \dots, u_M) = \|\pi(\mathbf{v}) - \pi(\mathbf{u_1} \wedge \cdots \wedge \mathbf{u_M})\|^2$$

on $|u_1| = \cdots = |u_M| = 1$ is a rational function

$$f(u_1, \dots, u_M) = \frac{g(u_1, \dots, u_M)}{h(u_1, \dots, u_M)}.$$

The points P of $\mathcal{V}_{M,M}(C)$, satisfying $|u_1| = \cdots = |u_M| = 1$, and minimizing the squared Hermitian distance are critical for f.

The proof is straightforward and resembles the one of Proposition 5. Moreover, the stationary points are solutions of a polynomial system of the same form of (14).

We can now formulate the Hermitian Minimum Distance from the Secant Variety (HMDSV) estimation algorithm for the DoAs. We search the point P of the secant variety $\mathcal{V}_{M,M}(C)$ that is closest to the point Q of the Grassmannian corresponding to the estimated signal subspace, with respect to the Hermitian distance:

Algorithm 4 Hermitian Minimum Distance from the Secant Variety (HMDSV)

1: compute the estimation $\widehat{V}$ of the signal subspace via PCA and compute first the Plücker coordinates defining Q, then $\pi(Q)$;
2: construct the affine coordinate $(s_1, \dots, s_{L'})$ of $\mathbf{u_1} \wedge \cdots \wedge \mathbf{u_M}$;
3: compute the rational function f described in Proposition 6 and its critical points by solving the corresponding polynomial system;
4: among the previous solutions, select the point P that minimize f. Finally, compute the estimation of the DoAs.

5. Numerical experiments

In this section, we apply the theoretical results of the previous sections to a simple example of DoAs estimation. We take the scenario with $L = 3$ sensors and $M = 2$ sources depicted in Fig. 2. The setup of the example assumes that the maximum amplitudes

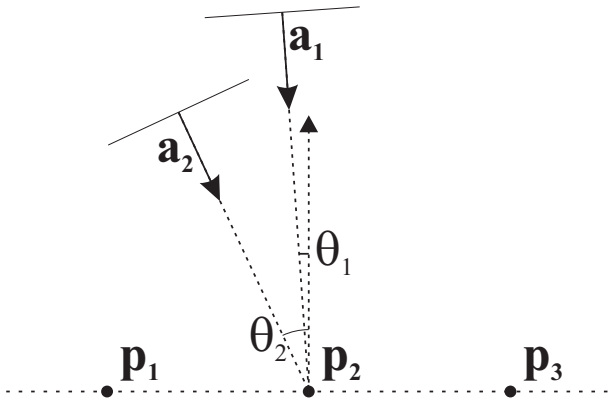

Figure 2. Representation of the numerical example: two planar waves, with orientations $\mathbf{a_1}$ and $\mathbf{a_2}$ defined by DoAs $\theta_1 = 4°$ and $\theta_2 = 25°$ respectively, are impinging on a ULA made of 3 antennas.

of the planar waves are $A_1 = 10$ and $A_2 = 12$, respectively. They can be assumed, in the slowly varying hypothesis, distributed according to an independent and identically distributed (i.i.d.) zero-mean white circularly-symmetric complex gaussian. Hence, the noiseless signal impinging on each element $\mathbf{p_l}$ of the antenna is, according to eq. (2) and eq. (3):

$$x_l(t) = s_{1,l}(t) + s_{2,l}(t) = s_1(t)\exp\left(-i\omega\tau_{1,l}(\mathbf{a}_1)\right) + s_2(t)\exp\left(-i\omega\tau_{1,l}(\mathbf{a}_2)\right),$$

where

$$s_m(t) \sim A_m\left(\mathcal{N}\left(0,\frac{1}{2}\right) + i\mathcal{N}\left(0,\frac{1}{2}\right)\right) = A_m\left(\mathcal{CN}(\mathbf{0},\mathbf{I}_N)\right). \tag{15}$$

In presence of noise, we assume ϵ_l to be additive complex following the same signal distribution but with a different variance σ^2 (equal for each antenna element).This means that the noisy signal is:

$$x_l(t) = s_1(t)\exp\left(-i\omega\tau_{1,l}(\mathbf{a}_1)\right) + s_2(t)\exp\left(-i\omega\tau_{1,l}(\mathbf{a}_2)\right) + \epsilon_l(t),$$

where

$$\epsilon_l(t) \sim \mathcal{N}\left(0,\frac{\sigma^2}{2}\right) + i\mathcal{N}\left(0,\frac{\sigma^2}{2}\right) = \sigma\left(\mathcal{CN}(\mathbf{0},\mathbf{I}_N)\right). \tag{16}$$

In this experiment we assume $\sigma = 20$.

The distance between two consecutive sensors is assumed to be equal to half wavelength, therefore:

$$d = |\mathbf{d}_{j,j+1}| = \frac{\lambda}{2} \quad \Rightarrow \quad z_m = \exp\left(-i\omega\tau_{j,j+1}(a_m)\right) = \exp\left(-ikd\sin\theta_m\right) = \exp\left(-i\pi\sin\theta_m\right).$$

Thus, the target solution (ideal and noiseless) for the DoAs θ_1, θ_2 are:

$$z_1 = 0.976 - 0.217i \qquad \text{and} \qquad z_2 = 0.241 - 0.971i.$$

In the following subsections we will show two simulations, firstly in a noiseless scenario and then in presence of noise. In both cases, we take $N = 1000$ snapshots of the same

signal. We did all the computations in MATLAB [20], but the solutions of the polynomial systems associated to FSMDSV and HMDSV algorithms, that have been calculated with MATHEMATICA [21]. The simplification of the two systems in the current scenario is reported in Appendix B.

5.1. **The noiseless scenario.** We apply the Principal Component Analysis to the noiseless measurements, obtaining orthonormal basis of the signal space V and its orthogonal complement $V^{\perp}$.

The polynomial (7) is calculated as explained in Section 4:

$$p(z) = (0.02 - 1.00\,i) + (-1.22 + 1.19\,i)z + z^2,$$

whose roots are z_1, z_2.

The polynomial (8) associated to the root-MUSIC algorithm is:

$$q(z) = (0.00 - 0.20\,i) + (-0.50 + 0.49\,i)z + z^2 + (-0.50 - 0.49\,i)z^3 + (0.00 + 0.20\,i)z^4,$$

whose roots are z_1, z_2, both with multiplicity two.

The polynomial (11) associated to the MDC algorithm is:

$$r(z) = (-0.01 + 0.41\,i) + (0.50 - 0.49\,i)z + (-0.50 - 0.49\,i)z^3 + (0.01 + 0.41\,i)z^4,$$

whose roots are z_1, z_2 and

$$z_3 = -0.716 + 0.699i, \qquad z_4 = 0.716 - 0.699i.$$

They are all unit complex numbers, however only z_1, z_2 satisfy inequality (12). Indeed, they are the minimum points of $d(\mathbf{z}, V)^2$, where the Hermitian distance is equal to zero.

Now, let us consider the polynomial system (17) defining the FSMDSV algorithm. By substituting into (v_0, v_1, v_2) the Plücker coordinates of V, we obtain:

$$\begin{cases} (-0.50 + 0.49\,i) - 0.77u_1 - 0.77u_2 + (0.50 + 0.49\,i)u_1^2 + (0.50 + 0.49\,i)u_1u_2 \\ +(0.50 + 0.49\,i)u_2^2 + (0.01 + 0.41\,i)u_1^2u_2 + (0.01 + 0.41\,i)u_1u_2^2 = 0 \\ (-0.20 + 0.20\,i) - 0.32u_1 - 0.32u_2 + (0.20 + 0.20\,i)u_1^2 + (0.20 + 0.20\,i)u_1u_2 \\ +(0.20 + 0.20\,i)u_2^2 + (0.00 + 0.17\,i)u_1^2u_2 + (0.00 + 0.17\,i)u_1u_2^2 = 0 \end{cases}$$

The system is symmetric with respect to the exchange of u_1 and u_2, therefore if (u_1, u_2) is a solution, (u_2, u_1) is a solution too. If we only take one of them, we obtain 4 distinct solutions (u_1, u_2):

$$(-0.974 + 0.532\,i, 1.3420.311\,i), (-0.721 + 0.945\,i, 1.938 - 2.133\,i),$$
$$(-0.550 + 0.966\,i, -0.303 - 1.346\,i), (0.976 - 0.217\,i, 0.241 - 0.971\,i).$$

However, we have to exclude the solutions that do not satisfy $|u_1| = |u_2| = 1$. Therefore, it remains only the last one:

$$(u_1, u_2) = (0.976 - 0.217\,i, 0.241 - 0.971\,i) = (z_1, z_2).$$

Moreover, we observe that f is equal to 1 only in (z_1, z_2).

Finally, let us consider the polynomial system (18) defining the HMDSV algorithm:

$$\begin{cases} (-1.22 + 1.19\,i) + 2u_1 + 2u_2 - (1.22 + 1.19\,i)u_1u_2 = 0 \\ -(8.39 + 8.19\,i)u_1 - (8.39 + 8.19\,i)u_2 + (0.17 + 6.89\,i)u_1^2 \\ +(0.33 + 13.78\,i)u_1u_2 + (0.17 + 6.89\,i)u_2^2 = 0 \end{cases}$$

whose solutions are $(-0.716 + 0.699\,i, 0.716 - 0.699\,i), (0.976 - 0.217\,i, 0.241 - 0.971\,i)$. The solution that minimizes the Hermitian distance is again:

$$(u_1, u_2) = (0.976 - 0.217\,i, 0.241 - 0.971\,i) = (z_1, z_2).$$

5.2. **A noisy scenario.** We apply the Principal Component Analysis to the noisy measurements, obtaining orthonormal basis of the estimated signal space $\widehat{V}$ and its orthogonal complement $\widehat{V}^{\perp}$.

If we apply the method explained in Section 4, we obtain an estimation of the polynomial $p(z)$:

$$\widehat{p}(z) = (0.25 - 1.01\,i) + (-1.23 + 1.16\,i)z + z^2,$$

whose roots are

$$\widehat{z}_1 = 0.891 - 0.050\,i, \qquad \widehat{z}_2 = 0.342 - 1.110\,i.$$

The estimated DoAs are

$$\widehat{\theta}_1 = 1.021 \qquad \text{and} \qquad \widehat{\theta}_2 = 23.887.$$

The estimation of the polynomial (8) is:

$$\widehat{q}(z) = (0.05 - 0.20\,i) + (-0.55 + 0.43\,i)z + z^2 + (-0.55 - 0.43\,i)z^3 + (0.05 + 0.20\,i)z^4,$$

whose roots are

$$\widehat{z}_{11} = 0.891 - 0.050\,i, \quad \widehat{z}_{12} = 1.119 - 0.063\,i, \quad \widehat{z}_{21} = 0.342 - 1.110\,i, \quad \widehat{z}_{22} = 0.253 - 0.823\,i.$$

Let us observe that $\widehat{z}_{11}$ and $\widehat{z}_{12}$ are approximately reciprocal number, such as $\widehat{z}_{21}$ and $\widehat{z}_{22}$. By taking their means and then their phases, we can compute the root-MUSIC estimation of the DoAs:

$$\widehat{\theta}_1 = 1.021 \qquad \text{and} \qquad \widehat{\theta}_2 = 23.887.$$

We obtained the same estimation given by the roots of $\widehat{p}(z)$.

The estimation of the polynomial (11) is:

$$\widehat{r}(z) = (-0.10 + 0.41\,i) + (0.55 - 0.43\,i)z + (-0.55 - 0.43\,i)z^3 + (0.10 + 0.41\,i)z^4,$$

whose roots are

$$\widehat{z}_1 = 0.998 - 0.065\,i, \quad \widehat{z}_2 = 0.310 - 0.951\,i, \quad \widehat{z}_3 = -0.788 + 0.616\,i, \quad \widehat{z}_4 = 0.788 - 0.616\,i.$$

Again, only $\widehat{z}_1, \widehat{z}_2$ satisfy inequality (12) and lie exactly on the unit circle. They are the minimum local points of $d(\mathbf{z}, V)^2$. The MDC estimation of the DoAs is:

$$\widehat{\theta}_1 = 1.191 \qquad \text{and} \qquad \widehat{\theta}_2 = 23.561.$$

Now, we take the estimation of the polynomial system (14) of FSMDSV:

$$\begin{cases} (-0.55 + 0.43\,i) - 0.74u_1 - 0.74u_2 + (0.55 + 0.43\,i)u_1^2 + (0.55 + 0.43\,i)u_1u_2 \\ +(0.55 + 0.43\,i)u_2^2 + (0.10 + 0.41\,i)u_1^2u_2 + (0.10 + 0.41\,i)u_1u_2^2 = 0 \\ (-0.23 + 0.18\,i) - 0.31u_1 - 0.31u_2 + (0.23 + 0.18\,i)u_1^2 + (0.23 + 0.18\,i)u_1u_2 \\ +(0.23 + 0.18\,i)u_2^2 + (0.04 + 0.17\,i)u_1^2u_2 + (0.04 + 0.17\,i)u_1u_2^2 = 0 \end{cases}$$

As in the noiseless scenario, the system is symmetric with respect to the exchange of u_1 and u_2, therefore if (u_1, u_2) is a solution, (u_2, u_1) is a solution too. If we only take one of them, we obtain 4 distinct solutions (u_1, u_2):

$$((-0.010 - 1.825\,i) \cdot 10^7, (0.010 + 1.825\,i) \cdot 10^7), (-1.000 + 0.025\,i, 0.375 + 0.927\,i),$$
$$(-0.738 + 0.675\,i, 0.562 - 0.827\,i), (0.997 - 0.074\,i, 0.314 - 0.950\,i).$$

Among the three solutions that satisfy $|u_1| = |u_2| = 1$, the last one maximizes f. So, the estimated roots are:

$$(u_1, u_2) = (0.997 - 0.74\,i, 0.314 - 0.950\,i) = (\widehat{z}_1, \widehat{z}_2).$$

For this pair, f is equal to 0.998. The FSMDSV estimation of the DoAs is:

$$\widehat{\theta}_1 = 1.358 \qquad \text{and} \qquad \widehat{\theta}_2 = 23.482.$$

Lastly, we compute the critical points for the HMDSV. In this case, the system is

$$\begin{cases} (-1.23+1.15\,i)+2u_1+2u_2-(1.23+1.16\,i)u_1u_2=0 \\ (0-1.07\,i)-(9.42+7.13\,i)u_1-(9.42+7.13\,i)u_2+(1.17+6.88\,i)u_1^2 \\ +(2.34+13.77\,i)u_1u_2+(1.17+6.88\,i)u_2^2=0 \end{cases}$$

whose solutions are $(-0.793+0.610\,i, 0.734-0.679\,i), (0.991-0.136\,i, 0.301-0.954\,i)$. The solution that minimize the distance is:

$$(u_1,u_2)=(0.991-0.136\,i, 0.301-0.954\,i)=(\widehat{z}_1,\widehat{z}_2).$$

The HMDSV estimation of the DoAs is:

$$\widehat{\theta}_1=2.497 \qquad \text{and} \qquad \widehat{\theta}_2=23.752.$$

Based on these examples, we can say that each method defines a consistent estimator. In the next section we show a further performance analysis of the proposed approaches against the root-MUSIC method.

6. Performance Analysis

In order to analyze the performances of the proposed approaches, we consider again a configuration of three antennas and two sources, as depicted in Fig. 2. In the first set of simulations, we assume that the sources are placed at $\pm\theta$ with respect to the array normal direction, where θ ranges from 1° to 20°. According to eq. 15 and 16 both the signal and the noise are assumed to be independent and identically distributed (i.i.d.) zero-mean white circularly-symmetric complex Gaussian. In order to analyze the performances of the proposed approach we keep unitary the signal variance varying the noise power, i.e. $s_m(t)\sim\mathcal{CN}(\mathbf{0},\mathbf{I}_N)$ and $\epsilon_l(t)\sim\sigma(\mathcal{CN}(\mathbf{0},\mathbf{I}_N))$. The SNR in decibel can then be defined as

$$SNR=10\log_{10}\left(\frac{\mathbb{E}\{s_m(t)\}}{\mathbb{E}\{\epsilon(t)\}}\right)=10\log_{10}\left(\frac{1}{\sigma^2}\right).$$

In Fig. 3 we show the accuracy of every method varying the SNR from 30dB to -20dB (worst condition), assuming that both sources have the same amplitude. For every θ and SNR we simulate 1000 signal acquisitions, each one composed by 1000 snapshots. In the left column of Fig. 3 we show the sample mean of each method, while on the right there is the corresponding sample standard deviation. We skip the graphics for the Plücker algorithm since, for the specific case of three antennas and two sources, this method defines exactly the same estimation of root-MUSIC, even if polynomial (13) is half-degree with respect to polynomial (9). As can be seen, for low values of SNR (depending on θ) the MDC method outperforms root-MUSIC and the other proposed algorithms, with respect to both the sample mean and the sample standard deviation.

In Fig. 4 we compare the behavior of the different approaches for $\theta=1°$, which is the most difficult condition for a proper DoAs estimation. As can be seen, in this scenario the MDC method is the most accurate for SNR smaller than 24dB.

In the last set of simulations, we set $\theta=1°$ and SNR equal to 10dB. We analyze the performances of the different estimators with respect to the number of snapshots adopted. In each configuration, we simulate 1000 acquisitions. The results are depicted in Fig. 5. The MDC method greatly outperforms the others, from a small number of snapshots up to more than 7000, both for the bias and for the sample standard deviation.

7. Conclusions

In this manuscript, we studied the problem of determining DoAs of a signal based on the measurements taken by a ULA of sensors. We showed how this problem is related to the geometry of the rational normal curve and its secant variety. Based on our analysis, we gave a geometrical interpretation of the classical root-MUSIC estimation algorithm. Then, we proposed some novel estimation methods based on subspace analysis. We presented a numerical simulation of localization problem with noisy measurements, that showed as all these methods have the potential to define good estimators of the DoAs. Furthermore, we performed a preliminary statistical analysis over the presented methods, checking their capability to estimate the correct DoAs in different SNR conditions and with a variable number of snapshots. The MDC approach outperforms the root-MUSIC method in most of cases, especially in low SNR contexts.

In an ongoing work, we are carrying out a complete statistical comparison of these methods. This will cover the statistical efficiency of the various estimators as well their computational complexity, as functions of the numbers L of sensors and M of sources. Moreover, we will focus on their resolution capability, i.e. the ability to distinguish between very close angles, and their robustness with respect to outliers. At this respect, the MDC, FSMDSV and HMDSV algorithms are very promising, since one could use the distances of the estimated points from the respective geometric sets as test statistic for the goodness of the estimation [22].

Acknowledgements

R. Notari is member of GNSAGA of INdAM.

Appendix A. A brief summary of projective geometry

Since the DoA model sits into telecommunication realm, and, in general, researchers in that field are not familiar with algebraic geometry, in this section we give a few details on projective spaces, rational normal curves and their secant varieties. This section can be skipped from readers who are aware of these topics. The exposition is largely inspired to [23].

A.1. **The projective space associated to a vector space.** Let W be a $(n+1)$-dimensional $\mathbb{K}$-vector space, and let $\mathcal{B}$ be a basis of W. The projective space $\mathbb{P}(W)$ associated to W is the set of 1-dimensional subspaces of W. These subspaces are called points of $\mathbb{P}(W)$.

Two non-zero vectors $\mathbf{v_1}, \mathbf{v_2}$ in W span the same 1-dimensional subspace if and only if their components $[\mathbf{v_1}]_{\mathcal{B}}, [\mathbf{v_2}]_{\mathcal{B}}$ with respect to $\mathcal{B}$ differ by a multiplicative non-zero scalar. The homogeneous coordinates of a point in $\mathbb{P}(W)$ are defined as the components of any non-zero vector in the corresponding subspace. Because of the previous property, homogeneous coordinates are defined up to a non–zero multiplicative scalar. Usually, homogeneous coordinates are written as $[x_0 : \cdots : x_n]$. Once we have chosen homogeneous coordinates, we switch notation from $\mathbb{P}(W)$ to $\mathbb{P}^n_{\mathbb{K}}$, to stress that we identify points by means of their homogeneous coordinates.

Another construction of projective spaces consists in joining the so–called ideal points to the points of an affine space. The relationship between the two construction is the following. Consider the set U_0 of points in $\mathbb{P}^n_{\mathbb{K}}$ whose homogeneous coordinates $[x_0 : x_1 :$

$\cdots : x_n]$ satisfy the condition $x_0 \neq 0$. Then, the map

$$F : U_0 \to \mathbb{A}^n_{\mathbb{K}}, \qquad F([x_0 : x_1 : \cdots : x_n]) = \left(\frac{x_1}{x_0}, \ldots, \frac{x_n}{x_0}\right)$$

is 1–to–1. In fact, the inverse of F is

$$F^{-1}(y_1, \ldots, y_n) = [1 : y_1 : \cdots : y_n].$$

So, one can identify U_0 with $\mathbb{A}^n_{\mathbb{K}}$. Points in $\mathbb{P}^n_{\mathbb{K}} \setminus U_0$ are thought of as ideal points of the affine space $\mathbb{A}^n_{\mathbb{K}}$, that is to say, directions of lines in $\mathbb{A}^n_{\mathbb{K}}$. Of course, an analogous invertible map can be constructed between $\mathbb{A}^n_{\mathbb{K}}$ and $U_j = \{[x_0 : \cdots : x_n] \mid x_j \neq 0\}$, for any $j = 1, \ldots, n$.

An isomorphism of the vector space W induces an isomorphism of $\mathbb{P}(W)$, that is called homography. The set of homographies is a group with respect to composition. Once we work with homogeneous coordinates, this group can be identified with $PGL_n(\mathbb{K})$, that consists of equivalence classes of invertible matrices of order $n+1$, where $\mathbf{A}, \mathbf{B}$ are in the same equivalence class if $\mathbf{A} = c\,\mathbf{B}$ for a suitable $c \in \mathbb{K}^*$. $PGL_n(\mathbb{K})$ is a multiplicative group, and acts on $\mathbb{P}^n_{\mathbb{K}}$. To geometrically explain the action, we have to define linear independence for points in projective spaces.

Definition 2. *The points $P_1, \ldots, P_s \in \mathbb{P}(W)$ are linearly independent if the sum of the associated 1–dimensional subspaces in W has dimension s.*

Theorem 2. *Let $\{P_0, \ldots, P_{n+1}\}, \{Q_0, \ldots, Q_{n+1}\}$ be two sets of points in $\mathbb{P}^n_{\mathbb{K}}$. There exists a unique matrix $\mathbf{R} \in PGL_n(\mathbb{C})$ such that $\mathbf{R}(P_j) = Q_j$ for $j = 0, \ldots, n+1$ if and only if every $n+1$ points in both sets are linearly independent.*

Finally, if the vector space W is endowed with a Euclidean or Hermitian structure, we can define a metric structure on $\mathbb{P}(W)$. Let us take two points P_1, P_2 in the projective space, correspondig to the subspaces of W generated by vectors $\mathbf{v_1}, \mathbf{v_2}$, respectively. The Fubini-Study distance between them is

$$d(P_1, P_2) = \arccos\left(\frac{|\langle \mathbf{v_1}, \mathbf{v_2}\rangle|}{\|\mathbf{v_1}\|\|\mathbf{v_2}\|}\right).$$

In the Euclidean case, the Fubini-Study distance corresponds to the angle between the two suspaces.

A.2. **Projective varieties and the rational normal curve.** Objects of interest in a projective space are projective varieties, defined as zero sets of a collection of homogeneous polynomials in $n+1$ variables. Homogeneous polynomials are needed, because a polynomial q vanishes at a point $[x_0 : \cdots : x_n]$ if $q(cx_0, \ldots, cx_n) = 0$ for every $c \in \mathbb{K}^*$. Two projective varieties X, Y in $\mathbb{P}^n_{\mathbb{K}}$ are projectively equivalent if there exists $\mathbf{R} \in PGL_n(\mathbb{C})$ such that $Y = \mathbf{R}(X)$. Usually, projective varieties are studied up to projective equivalence.

Linear subspaces in W are examples of projective varieties. In fact, a linear subspace contains vectors that are solutions of a homogeneous linear system. Moreover, if a non–zero vector is a solution, then also the 1–dimensional subspace it spans is contained into the solutions, and so they are projective varieties, as claimed.

The next example of projective variety is the main object of interest for studying the DoA model. In the following, we take $\mathbb{K} = \mathbb{C}$.

Definition 3. *Let $\mathbb{P}^n_{\mathbb{C}}$ be the complex projective space of dimension n. The rational normal curve $C \subseteq \mathbb{P}^n_{\mathbb{C}}$ is the image of*

$$v_n : \mathbb{P}^1 \hookrightarrow \mathbb{P}^n, \qquad v_n([t : u]) = [t^n : t^{n-1}u : \cdots : u^n].$$

The map v_n is called Veronese embedding of $\mathbb{P}^1$ into $\mathbb{P}^n$. When $PGL_1(\mathbb{C})$ acts on $\mathbb{P}^1_{\mathbb{C}}$, we get the same rational normal curve, but its points are parameterized in a different fashion. If we let $PGL_n(\mathbb{C})$ act on $\mathbb{P}^n_{\mathbb{C}}$, the rational normal curve is transformed in a projectively equivalent curve, called rational normal curve as well. If we choose a basis $a_0, \ldots, a_n$ of the homogeneous degree n polynomials in $\mathbb{C}[t, u]$, different from $t^n, t^{n-1}u, \ldots, u^n$, and we take the points $[a_0(t : u) : \cdots : a_n(t : u)]$, they form a rational normal curve. In fact, there exists a base change matrix $\mathbf{R}$ that transforms $t^n, \ldots, u^n$ in $a_0, \ldots, a_n$. Its equivalence class in $PGL_n(\mathbb{C})$ acts on $v_n(\mathbb{P}^1)$ and transforms it into $[a_0(t : u) : \cdots : a_n(t : u)]$, as claimed.

If X is a projective variety, the set of homogeneous polynomials that vanish at every point of X form the ideal $I(X)$ in the polynomial ring $\mathbb{C}[x_0, \ldots, x_n]$, that is called the defining ideal of X.

Proposition 7. *The defining ideal $I(C) \subseteq \mathbb{C}[z_0, z_1, \ldots, z_n]$ of the rational normal curve $C = v_n(\mathbb{P}^1_{\mathbb{C}})$ is generated by the 2×2 minors of the matrix*

$$\begin{bmatrix} z_0 & z_1 & \cdots & z_{n-1} \\ z_1 & z_2 & \cdots & z_n \end{bmatrix}.$$

Example 1. Plane conics are the rational normal curves in $\mathbb{P}^2_{\mathbb{C}}$. In fact, every conic, neither union of two lines, nor a double line, is defined by the vanishing of an irreducible, homogeneous, degree 2 polynomial. By a suitable change of coordinates, such a polynomial can be rewritten as $z_0z_2 - z_1^2$, that is the determinant of

$$\begin{bmatrix} z_0 & z_1 \\ z_1 & z_2 \end{bmatrix},$$

and so it is a rational normal curve. Hence, an irreducible and reduced conic is a rational normal curve, because it can be obtained from $z_0z_2 - z_1^2 = 0$ by the action of $PGL_2(\mathbb{C})$.

Example 2. In $\mathbb{P}^3_{\mathbb{C}}$, the rational normal curve is the twisted cubic, parameterized as $(t^3 : t^2u : tu^2 : u^3)$, and defined as the locus where $z_0z_2 - z_1^2, z_0z_3 - z_1z_2, z_1z_3 - z_2^2$ vanish. No two of the three quadrics are enough to cut the twisted cubic, because every two of them have a line in common, other than the twisted cubic.

For the study of the DoA model, a very important property of rational normal curves is the following.

Proposition 8. *Let $C = v_n(\mathbb{P}^1_{\mathbb{C}})$ be the rational normal curve, and let $P_0, \ldots, P_n \in C$. Then, $P_0, \ldots, P_n$ are pairwise distinct points if and only if they are linearly independent.*

A quite subtle property of rational normal curves is that they are the only curves for which this property holds.

A final interesting property of rational normal curves is the one described in the Castelnuovo's Lemma. To get an irreducible and reduced plane conic, one has to choose 5 points in $\mathbb{P}^2_{\mathbb{C}}$, no three on the same line. A similar question can be asked for every other rational normal curve, and can be considered as an interpolation problem in projective spaces. Even if we do not have to construct rational normal curves to study the DoA model, we quote the solution of the above problem.

Theorem 3 (Castelnuovo's Lemma)**.** *Through any $n+3$ points in general position in $\mathbb{P}^n_{\mathbb{C}}$ there passes a unique rational normal curve.*

A.3. **Grassmannians and secant varieties.** The solution of the DoA model can be rephrased in terms of linear subspaces of dimension M that meet the rational normal curve at M different points. Thus, it is useful to introduce Grasmmannian varieties and secant varieties to the rational normal curve therein.

Definition 4. *The Grassmannian variety $\mathbb{G}(M, W)$ is the set whose points are the M-dimensional linear subspaces of the vector space W.*

Of course, $\mathbb{G}(1, W) = \mathbb{P}(W)$. In this respect, Grassmannian varieties can be thought of as generalizations of projective spaces.

Grassmannians can also be seen as projective varieties. Given W, let us construct its M–th exterior power $\wedge^M W$ as the vector space whose elements are linear combinations of $\mathbf{w_1} \wedge \cdots \wedge \mathbf{w_M}$, where $\mathbf{w_1}, \ldots, \mathbf{w_M} \in W$.[4] If $U \subset W$ is an M–dimensional subspace with bases $(\mathbf{u_1}, \ldots, \mathbf{u_M})$, $(\mathbf{u'_1}, \ldots, \mathbf{u'_M})$, then $\mathbf{u_1} \wedge \cdots \wedge \mathbf{u_M}$ and $\mathbf{u'_1} \wedge \cdots \wedge \mathbf{u'_M}$ differ only by a scalar, i.e. the determinant of the base change matrix. This means that they are the same point in $\mathbb{P}(\wedge^M W)$. So, we can think to $\mathbb{G}(M, W)$ as a subset of $\mathbb{P}(\wedge^M W)$. More precisely, $\mathbb{G}(M, W)$ is embedded into $\mathbb{P}(\wedge^M W)$ via the Plücker embedding:

$$\begin{array}{ccc} \mathbb{G}(M, W) & \hookrightarrow & \mathbb{P}(\wedge^M W) \\ U & \mapsto & [\mathbf{u_1} \wedge \cdots \wedge \mathbf{u_M}] \end{array} .$$

Given a basis $\mathcal{B} = (\mathbf{e_0}, \ldots, \mathbf{e_n})$ of W, the associated basis in $\wedge^M W$ and the corresponding reference frame in $\mathbb{P}(\wedge^M W)$ is

$$\mathcal{B}^{\mathcal{M}} = ((-1)^{\epsilon_{I,J}} \mathbf{e_{i_1}} \wedge \cdots \wedge \mathbf{e_{i_M}} \mid 0 \leq i_1 < \cdots < i_M \leq n),$$

where $I = \{i_1, \ldots, i_M\}, J = \{0, \ldots, n\} \setminus I$, and $\epsilon_{I,J}$ is the parity of the permutation I, J of $\{0, \ldots, n\}$. The associated homogeneous coordinates are called Plücker coordinates. If W is an Euclidean or Hermitian space and $\mathcal{B}$ is orthonormal, then the induced structure on $\wedge^M W$ is the one where $\mathcal{B}^{\mathcal{M}}$ is orthonormal. This way it is also possible to define the Fubini-Study metric on $\mathbb{P}(\wedge^M W)$.

Finally, we are interested in defining varieties whose points are subspaces that meet the rational normal curve at a prescribed number of points. Such varieties are called secant varieties.

Definition 5. *Let $C \subset \mathbb{P}^n_{\mathbb{C}}$ be the rational normal curve and let k, k' be integers. The closure of the set of subspaces of W of dimension k and meeting C at k' distinct points is the variety $\mathcal{V}_{k,k'}(C)$, called k'–secant variety of k–subspaces.*

Since the points of the k'–secant variety of k–subspaces are subspaces of W of dimension k, we have $\mathcal{V}_{k,k'}(C) \subset \mathbb{G}(k, W)$. Because of Proposition 8, if $k = k'$ it is enough to take k distinct points on C to get a point in $\mathcal{V}_{k,k}(C)$. Hence, $\mathcal{V}_{k,k}(C) \subset \mathbb{G}(k, W)$ has dimension k, for every $k \leq n$.

Appendix B. The simplification of the polynomial systems

Here we sketch the simplifications for the polynomial systems associated to FSMDSV and HMDSV estimation algorithms, in the case $L = 3, M = 2$.

[4]Here, we do not give details on the construction of $\wedge^M W$ (see [24] for a comprehensive presentation or [25], Appendix A, for a short introduction). We only remark that $\wedge$ is linear with respect to the operations in W and skew–commutative.

B.1. **FSMDSV.** With the above numbers of sensors and sources, the rational function f of Proposition 5 is:

$$\begin{aligned} f(u_1,u_2) &= \frac{1}{u_1^2+4u_1u_2+u_2^2}\cdot\Big(\overline{v_2}v_0-(\overline{v_1}v_0+\overline{v_2}v_1)(u_1+u_2)+(|v_0|^2+|v_2|^2)u_1u_2+ \\ &\qquad |v_1|^2(u_1+u_2)^2-(\overline{v_0}v_1+\overline{v_1}v_2)u_1u_2(u_1+u_2)+\overline{v_0}v_2u_1^2u_2^2\Big) \\ &= \frac{g(u_1,u_2)}{h(u_1,u_2)}. \end{aligned}$$

Then, the associated polynomial system is:

$$\begin{cases} p_1(u_1,u_2) &= g(u_1,u_2)\,\dfrac{\partial h(u_1,u_2)}{\partial u_1}-h(u_1,u_2)\,\dfrac{\partial g(u_1,u_2)}{\partial u_1}=0 \\ p_2(u_1,u_2) &= g(u_1,u_2)\,\dfrac{\partial h(u_1,u_2)}{\partial u_2}-h(u_1,u_2)\,\dfrac{\partial g(u_1,u_2)}{\partial u_2}=0 \end{cases}.$$

Let us define:

$$\begin{aligned} q_1(u_1,u_2) &= \frac{u_1p_1(u_1,u_2)+u_2p_2(u_1,u_2)}{u_1^2+4u_1u_2+u_2^2}, \\ q_2(u_1,u_2) &= \frac{-(2u_1+u_2)p_1(u_1,u_2)+(u_1+2u_2)p_2(u_1,u_2)}{(u_1-u_2)(u_1^2+4u_1u_2+u_2^2)}, \\ q_3(u_1,u_2) &= (u_1+u_2)q_1(u_1,u_2)-u_1u_2\,q_2(u_1,u_2). \end{aligned}$$

The polynomial $q_1(u_1,u_2)$ and $q_3(u_1,u_2)$ have both degree 4, with the same leading monomial $u_1^2u_2^2$, but different leading coefficients. The following linear combination defines a degree 3 polynomial:

$$q_4(u_1,u_2)=(-v_0\overline{v_1}-v_1\overline{v_2})\,q_1(u_1,u_2)-2v_0\overline{v_2}\,q_3(u_1,u_2).$$

Since also $q_2(u_1,u_2)$ has degree 3, we obtained the following degree 9 polynomial system:

$$\begin{cases} q_2(u_1,u_2)=0 \\ q_4(u_1,u_2)=0 \end{cases}. \tag{17}$$

B.2. **HMDSV.** In our scenario, we have $\pi(\mathbf{u_1}\wedge\mathbf{u_2})=(-u_1-u_2,u_1u_2)$ and $\pi(\mathbf{v})=(v_1,v_2)$. Then,

$$\begin{aligned} &f(u_1,u_2)=(\overline{v_1+u_1+u_2})\;(v_1+u_1+u_2)+(\overline{v_2-u_1u_2})\;(v_2-u_1u_2)= \\ &=\frac{1}{u_1u_2}\left(-\overline{v_2}u_1^2u_2^2+\overline{v_1}u_1^2u_2+\overline{v_1}u_1u_2^2+u_1^2+\left(3+|v_1|^2+|v_2|^2\right)u_1u_2+u_2^2+v_1u_1+v_1u_2-v_2\right). \end{aligned}$$

The critical points of $f(u_1,u_2)$ are solutions of the system

$$\begin{cases} \tilde{q}_1(u_1,u_2)=-\overline{v_2}u_1^2u_2^2+\overline{v}_1u_1^2u_2+u_1^2-u_2^2-v_1u_2+v_2=0 \\ \tilde{q}_2(u_1,u_2)=-\overline{v_2}u_1^2u_2^2+\overline{v}_1u_1u_2^2-u_1^2+u_2^2-v_1u_1+v_2=0 \end{cases}.$$

We take the difference of the first and second polynomials and we divide by u_1-u_2. This is possible because we are looking for solutions that fulfil $u_1\neq u_2$. We get the third polynomial

$$\tilde{q}_3(u_1,u_2)=\overline{v_1}u_1u_2+2u_1+2u_2+v_1.$$

It is possible to further simplify the system by computing the remainder of the division between the first and third equation, and we get the forth polynomial

$$\tilde{q}_4(u_1,u_2)=-\left(\frac{\overline{v_1}^2+4\overline{v_2}}{\overline{v_1}^2}\right)\left((u_1+u_2)^2-v_1(u_1+u_2)+v_2+\frac{\overline{v_2}(v_1^2+4v_2)}{\overline{v_1}^2+4\overline{v_2}}\right).$$

Therefore, the critical points for $f(u_1, u_2)$ can be computed by solving the following degree 4 system:

$$\begin{cases} \tilde{q}_3(u_1, u_2) = 0 \\ \tilde{q}_4(u_1, u_2) = 0 \end{cases} \tag{18}$$

References

[1] A. Abdelbari and B. Bilgehan. A novel doa estimation method of several sources for 5g networks. In *2020 International Conference on Electrical, Communication, and Computer Engineering (ICECCE)*, pages 1–6, 2020.

[2] Y. Hu, T. D. Abhayapala, and P. Samarasinghe. Multiple source direction of arrival estimations using relative sound pressure based music. *IEEE/ACM Transactions on Audio, Speech, and Language Processing*, pages 1–1, 2020.

[3] Jian Li and Petre Stoica. Mimo radar with colocated antennas. *IEEE Signal Processing Magazine*, 24(5):106–114, 2007.

[4] Zahraa Jaafer, Salman Goli, and Amer Elameer. Best performance analysis of doa estimation algorithms. pages 235–239, 11 2018.

[5] Peter Gerstoft, Angeliki Xenaki, and Christoph F. Mecklenbräuker. Multiple and single snapshot compressive beamforming. *The Journal of the Acoustical Society of America*, 138(4):2003–2014, October 2015.

[6] H.L. Van Trees. *Optimum Array Processing – Part IV of Detection, Estimation, and Modulation Therory*. 05 2002.

[7] Leon Cohen. *Time-Frequency Analysis: Theory and Applications*. Prentice-Hall, Inc., USA, 1995.

[8] Athanassios Manikas. *Differential geometry in array processing*. Imperial College Press, London, 2004.

[9] Song Jie, Yang Fu-cheng, Cai Fu-qing, and Yu Yi-wei. Complex envelope estimation of direct-path pulse signal based on real data. In *International Conference on Radar Systems (Radar 2017)*, pages 1–5, 2017.

[10] Hendrik Kleene and Dirk Schulz. Concept of a complex envelope faber polynomial approach for the solution of maxwell's equations. In *2018 IEEE MTT-S International Conference on Numerical Electromagnetic and Multiphysics Modeling and Optimization (NEMO)*, pages 1–3, 2018.

[11] J. Capon. High-resolution frequency-wavenumber spectrum analysis. *Proceedings of the IEEE*, 57(8):1408–1418, 1969.

[12] Jon Petter Asen, Jo Inge Buskenes, Carl-Inge Colombo Nilsen, Andreas Austeng, and Sverre Holm. Implementing capon beamforming on a GPU for real-time cardiac ultrasound imaging. *IEEE Transactions on Ultrasonics, Ferroelectrics, and Frequency Control*, 61(1):76–85, January 2014.

[13] S. Moon, S. Lee, and I. Lee. Sum-rate capacity of random beamforming for multi-antenna broadcast channels with other cell interference. *IEEE Transactions on Wireless Communications*, 10(8):2440–2444, 2011.

[14] Di Shen, JieSheng Chen, and Jian Gong. Polynomial rooting algorithm for doa estimation based on signal subspace. In *2011 4th International Congress on Image and Signal Processing*, volume 5, pages 2617–2620, 2011.

[15] D. V. Sidorovich and A. B. Gershman. Two-dimensional wideband interpolated root-music applied to measured seismic data. *IEEE Transactions on Signal Processing*, 46(8):2263–2267, 1998.

[16] F. Yan, X. Li, T. Jin, L. Liu, and M. Jin. A real-valued polynomial rooting method for fast direction of arrival estimation with large uniform linear arrays. *IEEE Access*, 7:122330–122341, 2019.

[17] M. Pesavento, A. B. Gershman, and M. Haardt. Unitary root-music with a real-valued eigendecomposition: a theoretical and experimental performance study. *IEEE Transactions on Signal Processing*, 48(5):1306–1314, 2000.

[18] M. Wagner, Y. Park, and P. Gerstoft. Gridless doa estimation and root-music for non-uniform linear arrays. *IEEE Transactions on Signal Processing*, 69:2144–2157, 2021.

[19] E. R. Heineman. Generalized Vandermonde determinants. *Trans. Amer. Math. Soc.*, 31(3):464–476, 1929.

[20] MATLAB. version 9.7.0.1190202 (r2019b), 2020.

[21] Wolfram Research, Inc. Mathematica, Version 12.3.1. Champaign, IL, 2021.

[22] Marco Compagnoni, Alessia Pini, Antonio Canclini, Paolo Bestagini, Fabio Antonacci, Stefano Tubaro, and Augusto Sarti. A geometrical–statistical approach to outlier removal for tdoa measurements. *IEEE Transactions on Signal Processing*, 65(15):3960–3975, 2017.

[23] Joe Harris. *Algebraic geometry*, volume 133 of *Graduate Texts in Mathematics*. Springer-Verlag, New York, 1995. A first course, Corrected reprint of the 1992 original.

[24] Werner Greub. *Multilinear algebra*. Universitext. Springer-Verlag, New York-Heidelberg, second edition, 1978.

[25] M. Compagnoni, R. Notari, F. Antonacci, and A. Sarti. A comprehensive analysis of the geometry of tdoa maps in localization problems. *Inverse Problems*, 30(3), 2014.

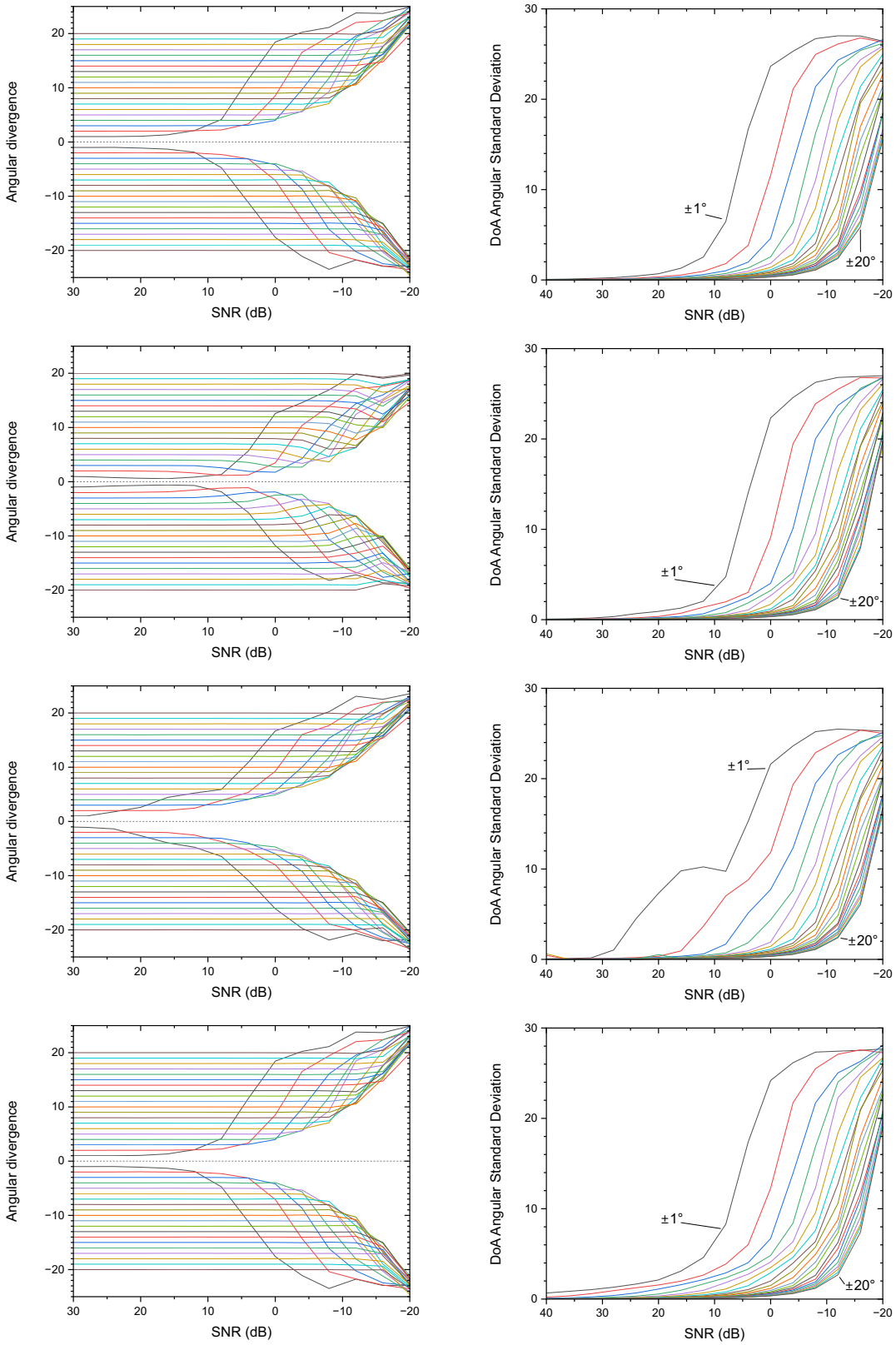

FIGURE 3. Comparison of the proposed methods for different angular distance of the two sources. From the first row to the last one: root-MUSIC, MDC, FSMDSV and HMDSV are compared as function of the SNR. In the first column we report the sample mean values of the estimated DoAs, while in the second column we provide their sample standard deviations.

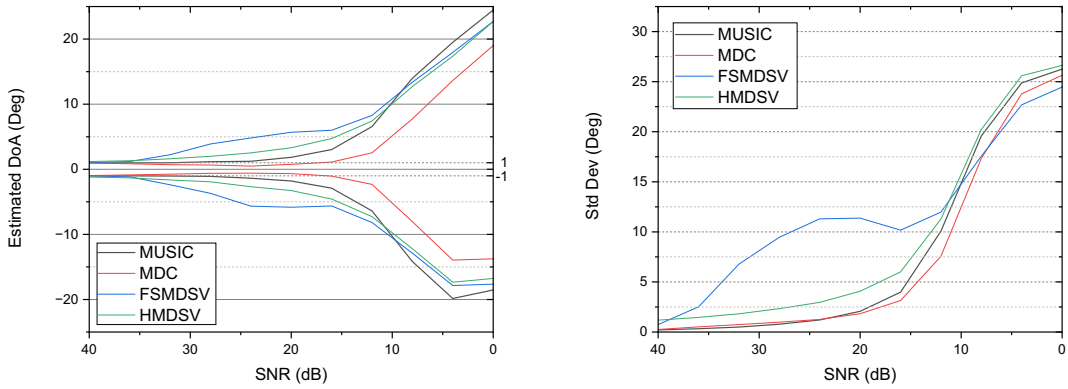

FIGURE 4. Comparison of the proposed methods for two sources at $\pm 1^\circ$ as a function of the SNR. On the left: the sample mean of the estimated DoAs. On the right: their sample standard deviation.

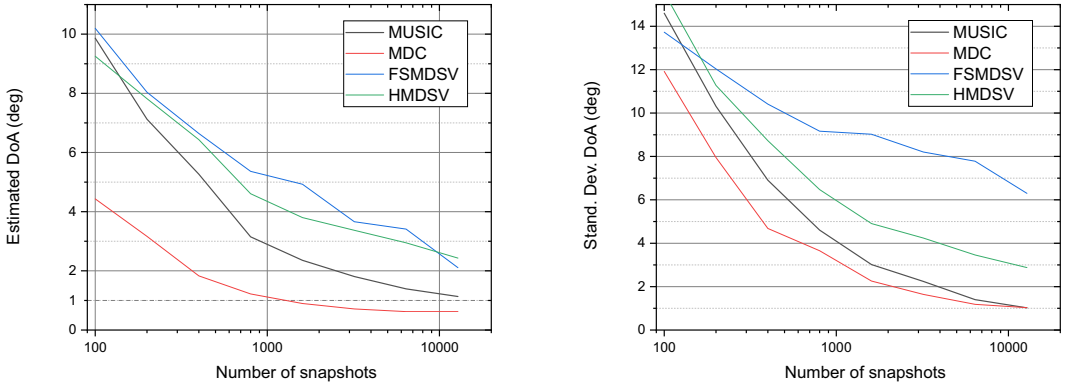

FIGURE 5. Comparison of the proposed methods for two sources at $\pm 1^\circ$ and SNR equal to 10dB, with a varying number of snapshots. On the left: the sample mean. On the right: their sample standard deviation.